An Electron Microscopic Study on the Crystallization of Amorphous Ti-(Fe, Co or Ni)-B Alloys

An Electron Microscopic Study on the Crystallization of Amorphous Ti-(Fe, Co or Ni)-B Alloys*

C. Suryanarayana**, Akihisa Inoue

and Tsuyoshi Masumoto

The Research Institute for Iron, Steel and Other Metals

(Received January 24, 1980)

Synopsis

By rapidly quenching melts of ternary Ti-X-B (X=Fe, Co or Ni) with a melt spinning apparatus, it has been possible to produce amorphous phases. X-ray and electron diffraction studies confirmed the nature of the amorphous phase. Crystallization studies of the amorphous phase have been carried out with a transmission electron microscope. Both in situ studies and investigations on samples annealed externally at temperatures determined by D.T.A., aided in establishing a general sequence for the crystallization behavior. All the amorphous alloys initially transformed to a metastable b.c.c. supersaturated solid solution of Ti followed by the precipitation of the equilibrium cubic intermetallic compound Ti_2X. Differences between the two approaches of crystallization studies are highlighted.

I. Introduction

Amorphous metals or metallic glasses have been the subject of intensive research in recent years[1-3]. These amorphous alloys are produced mostly by rapid quenching of their resepective melts at cooling rates exceeding about 10^5 K/s, and offer potential industrial applications[4,5]. However, for an efficient utilization of these metastable alloys, their stability as a function of temperature and time has to be ascertained. Further, as the properties of the amorphous alloys change with the onset of crystallization, the crystallization

---

* The 1707th report of the Research Institute for Iron, Steel and Other Metals.

** Permanent address: Department of Metallurgical Engineering, Banaras Hindu University, Varanasi-221005, India.

behavior of these alloys is expected to provide valuable information on the constitution and hence the change in their properties. We present here an electron microscopic study on the crystallization behavior of ternary $Ti_{70}X_{20}B_{10}$* (X=Fe, Co or Ni) amorphous alloys.

The constitution of these ternary alloys under equilibrium conditions is not well established. An isothermal section at 1273 K for the Ti-Fe-B system[6] and the isothermal sections at 1073 K for the Ti-Co-B[7] and Ti-Ni-B[8] systems only are available in literature. These isothermal sections indicate that for the compositions of our interest the equilibrium phases are the h.c.p. α-Ti solid solution, the f.c.c. Ti_2X (X=Fe, Co or Ni) intermetallic compound and the orthorhombic TiB phase. In the absence of any other data, it is assumed that the same constitution continues till room temperature.

II. Experimental Procedure

Ternary alloys of titanium with 10 atomic percent B and 20 atomic percent Fe, Co or Ni have been prepared by taking the appropriate quantities of the pure elements and melting them in an arc furnace under a protective argon atmosphere. The alloys have been repeatedly melted to ensure homogeneity. Long, uniform and continuous ribbons of these alloys were obtained using a specially designed melt spinning apparatus [9]. About 5g of the alloy was used per run and the speed of the copper roll was about 4000 r.p.m.

The amorphous nature of the ribbons was confirmed both by x-ray diffraction and electron microscopy. The crystallization temperatures (T_x) of the amorphous alloys were measured in a differential thermal analyzer (D.T.A.) by heating the foils at a constant rate of 8.33×10^{-2} K/s. Hardness of the amorphous alloys was measured by a Vickers hardness tester with a load of 100g.

Specimens heat treated for 600, 1800 and 3600 s at temperatures corresponding to T_x's have been observed in a JEM-200B transmission electron microscope operating at 200 kV after thinning the foils in an electrolyte consisting of 95 parts methanol and 5 parts sulphuric acid cooled to about 220 K[10]. Some thinned foils have also been crystallized in-situ in a Hitachi HU-11D 100 kV electron microscope using the hot stage.

---

* All compositions are expressed in atomic percent by subscripts.

III. Results and Discussion

Table 1 lists the crystallization temperatures and hardness values of the amorphous alloys obtained in this investigation. All the alloys exhibit two exothermic crystallization peaks indicating that crystallization is a two-stage process. Fig. 1 shows the D.T.A. curves. From these curves, it can be observed that the iron-containing alloy shows a small broad peak followed by a very narrow, high-intensity peak. On the other hand, the peaks in the other two alloys are broad and are of low intensity. This appears a little unusual.

Table I. Crystallization Tempratures and Hardness values of Amorphous $Ti_{70}X_{20}B_{10}$

Alloy	T_{x1}(K)	T_{x2}(K)	H_v(Kg/mm^2)
$Ti_{70}Fe_{20}B_{10}$	778	858	692
$Ti_{70}Co_{20}B_{10}$	713	777	659
$Ti_{70}Ni_{20}B_{10}$	768	793	626

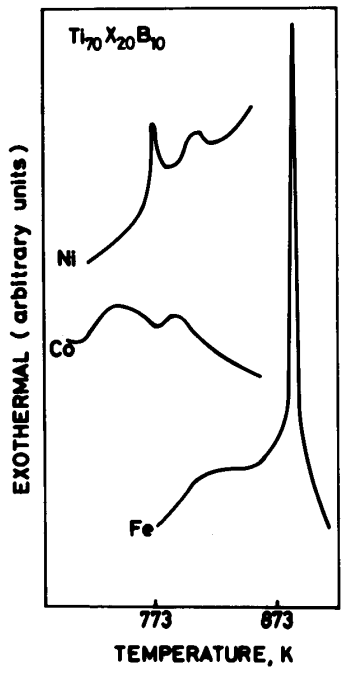

Fig. 1 D.T.A. Curves of the amorphous $Ti_{70}X_{20}B_{10}$ alloys.

Detailed electron microscopic investigations have been carried out to understand the decomposition behavior of the amorphous phase in these systems. For this purpose, two approaches have been undertaken. The first was continuous in-situ heating of the samples in a 100 kV microscope and follow the structural changes. On the other hand, the second approach was to heat treat amorphous foils for different times at temperatures corresponding to T_x's indicated by the D.T.A. curves and observe the thinned foils in a 200 kV microscope. Both the approaches gave essentially the same results. However, some possible sources of misinterpretation will be highlighted from the structural point of view.

Fig. 2 a shows the bright-field electron micrograph of the as-quenched $Ti_{70}Co_{20}B_{10}$ amorphous alloy and Fig. 2 b the corresponding diffraction pattern. The micrograph is featureless and the diffraction pattern shows only diffuse haloes, thus confirming the amorphous nature of the alloy. Dark-field micrographs taken from the first diffuse ring did not show any contrast due to the presence of any possible microcrystallites. Both iron-containing and nickel-containing alloys also exhibited similar features, suggesting that all the alloys could be completely solidified into the amorphous state by rapid quenching.

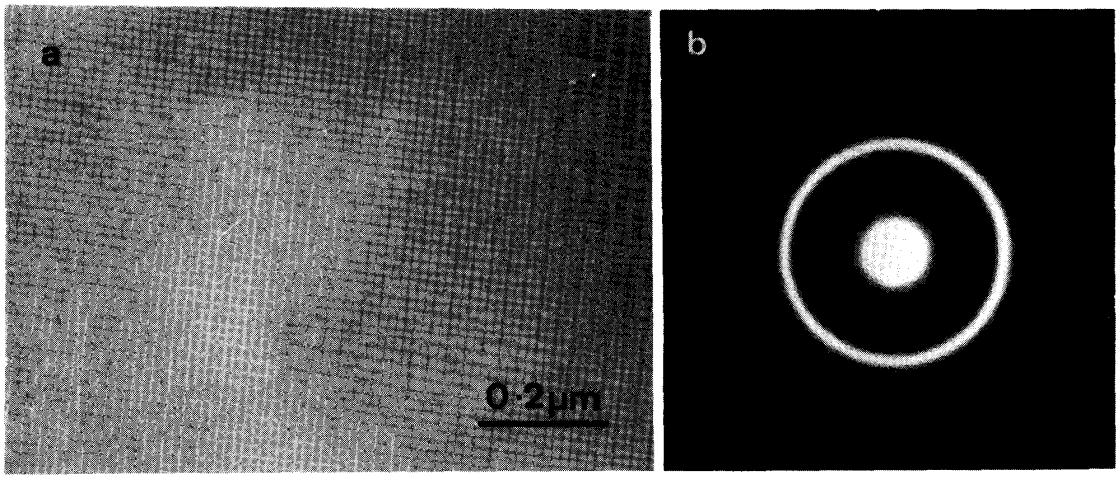

Fig. 2 (a) Bright-field electron micrograph and (b) Diffraction pattern of the as-quenched $Ti_{70}Co_{20}B_{10}$ alloy.

Although binary Ti-Ni alloys in a limited composition range have been reported to be amorphous by rapid quenching[11], it has been found very difficult to produce an amorphous phase in Ti-Fe and Ti-Co binary alloy[12]. On the other hand, it was noticed that the grain size de-

creased in the order Fe, Co and Ni reaching a size as small as 20 nm. However, the present results indicate that it is possible to produce an amorphous phase by the addition of about 10 at.% boron to the above binary alloys. Silicon was also found effective in promoting the formation of an amorphous phase[12, 13]

When the amorphous alloy specimens were heated in-situ in the electron microscope with the help of a hot stage, the amorphous phase continued to show lack of contrast in the bright-field micrograph until, when the temperature was continuously increased, crystallization started suddenly. Nucleation of the crystalline phase was very homogeneous and the particle size extremely small (Fig. 3 a). Fig. 3 b shows the selected area diffraction pattern obtained from this phase. Analysis of this diffraction pattern indicated that the precipitating phase had an f.c.c. structure with a lattice parameter $a \simeq 0.46$ nm. A phase with the same structure and almost the same lattice parameter was found in the Co- and Ni-containing alloys also. It should, however, be mentioned that the relative intensities of the reflections do not correspond to those expected from an f.c.c. structure.

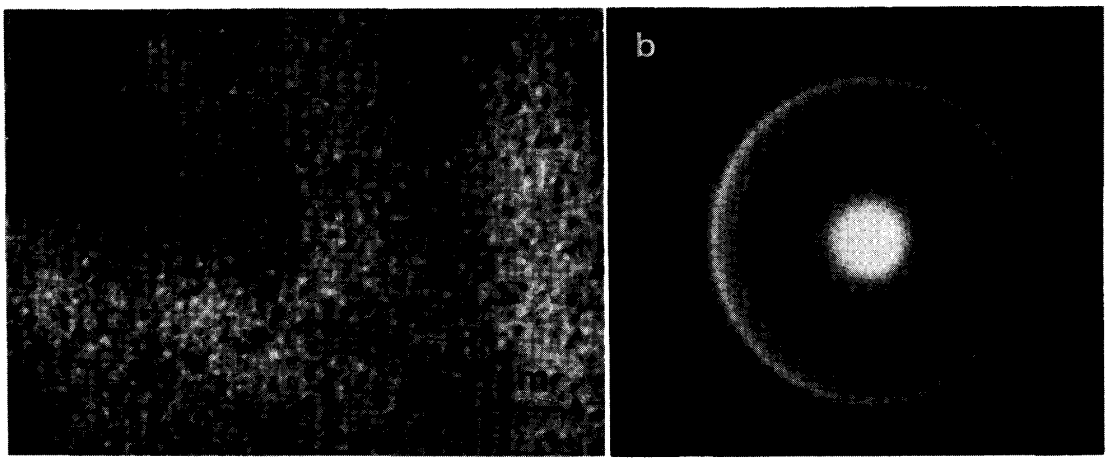

Fig. 3 (a) Bright-field micrograph of the in-situ crystallized $Ti_{70}Fe_{20}B_{10}$ alloy. (b) Diffraction pattern of above.

Neither the constituent binary diagrams nor the ternary diagrams involved in this study show the presence of any phase with this structure and lattice parameter. Therefore, this can be considered metastable. In general, it has been noticed during decomposition of amorphous phases that the first stage of crystallization is the formation of a supersaturated solid solution with the structure of the

solvent metal. Thus, f.c.c. solid solutions have been obtained in Pd- or Ni-base[14, 15], h.c.p. solid solutions in Co-base[16] and b.c.c. solid solutions in Fe-base[15] amorphous phases. Thus, one would have expected the formation of a metastable b.c.c. solid solution (based on the high-temperature polymorph of Ti) in these alloys. Therefore, the formation of an f.c.c. phase is surprising and quite unexpected.

In order to verify the above result and also to obtain detailed information on the decomposition sequence, the amorphous alloy foils have been heat treated for different times externally at temperatures corresponding to T_x's and observed in a 200 kV microscope.

Fig. 4 shows a bright-field electron micrograph and the corresponding diffraction pattern for the amorphous $Ti_{70}Co_{20}B_{10}$ alloy annealed for 1800 s at 713 K. The micrograph shows the precipitation of some tiny particles and the sharp diffraction lines show the existence of a crystalline phase with a b.c.c. structure. The lattice parameter calculated from this pattern is about 0.29 nm. It may be mentioned at this juncture that the diffraction pattern did not change appreciably even when the foils were annealed for 3600 s at 713 K. The small value of the lattice parameter suggests that this phase is either a highly supersaturated solid solution of Co and B in Ti or this could be the equilibrium CoTi phase. The latter possibility is unlikely because CoTi has an ordered b.c.c. (CsCl type) structure which should give rise to superlattice reflections of the type $h+k+1 \neq 2N$, where N is an integer. Such superlattice reflections were not observed in our diffraction patterns. Perhaps this is the first observation where such a highly supersaturated solid solution is precipitated from the amorphous phase. But, if one assumes that the amorphous phase is homo-

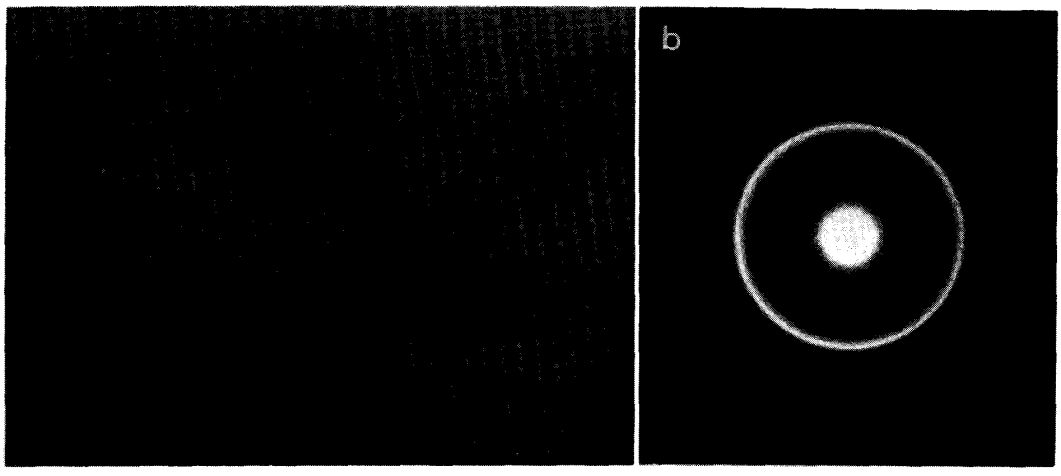

Fig. 4 (a) Electron micrograph of $Ti_{70}Co_{20}B_{10}$ alloy annealed for 1800 s at 713 K. (b) Diffraction Pattern of above.

geneous, then this observation may not be so surprising, since it had been shown earlier that very long annealing treatments at low temperatures transform the amorphous phase to a supersaturated solid solution 16).

However, when the foils were annealed at 777 K, one could detect the appearance of another crystalline phase. Figs. 5 a and b show the micrograph and diffraction pattern from the $Ti_{70}Co_{20}B_{10}$ alloy annealed for 3600 s at 777 K. The diffraction pattern could be satisfactorily indexed on the basis of a phase mixture consisting of Ti_2Co having an f.c.c. structure with a = 1.13 nm and TiB having an orthorhombic structure with a = 0.612, b = 0.306 and C = 0.2 nm. But when the foils were annealed at 777 K for only 600 s, we could detect only the Ti_2Co phase. Thus, one could conclude that the second phase to precipitate out of the amorphous matrix is the Ti_2Co phase. Subsequent heat treatments resulted in achieving the equilibrium constitution.

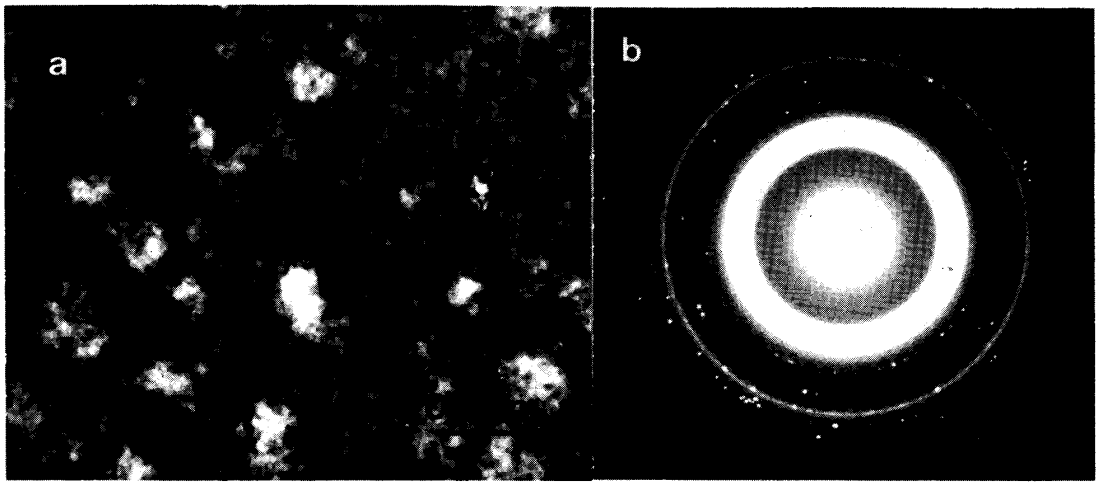

Fig. 5(a) Electron micrograph of $Ti_{70}Co_{20}B_{10}$ alloy annealed for 3600 s at 777 K showing the presence of the second phase. (b) Diffraction pattern of above.

Similar behavior of precipitation was observed for the Fe- and Ni-containing alloys also when annealed at temperatures corresponding to T_{x2}. The size of the precipitate is larger in the Ni-containing alloys, enabling us to record single-crystal electron diffraction patterns. Figs. 6 a and b show bright-field micrographs of heat treated $Ti_{70}Fe_{20}B_{10}$ and $Ti_{70}Ni_{20}B_{10}$ alloys. Fig. 7 shows the diffraction pattern of the $Ti_{70}Fe_{20}B_{10}$ alloy and its analysis is shown in Table II. Fig. 8 shows three different orientations of the Ti_2Ni phase in the $Ti_{70}Ni_{20}B_{10}$ alloy.

Thus, heat treatments carried out externally on the amorphous

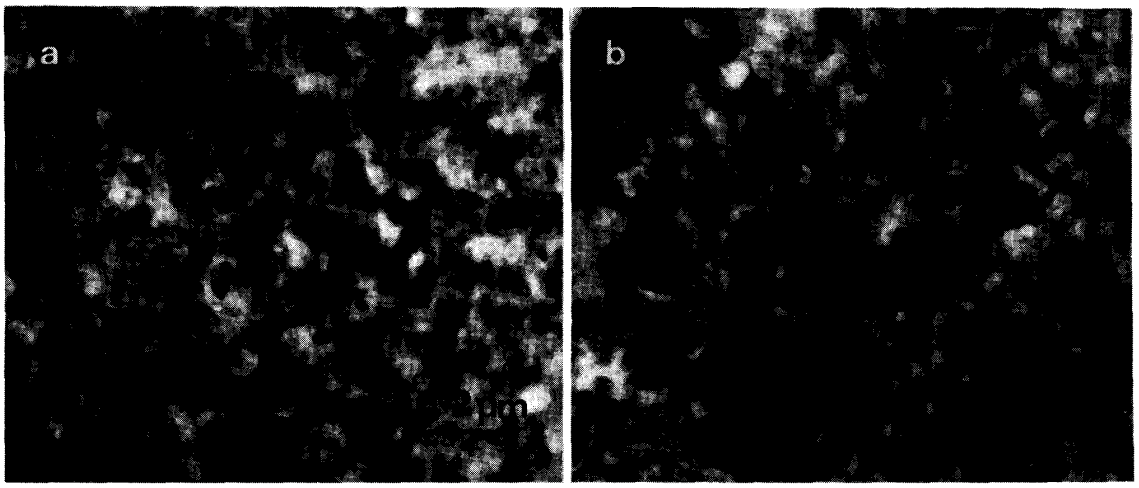

Fig. 6 Bright-field electron micrographs of foils heat treated to produce the crystalline in termediate phase. (a) $Ti_{70}Fe_{20}B_{10}$ (b) $Ti_{70}Ni_{20}B_{10}$.

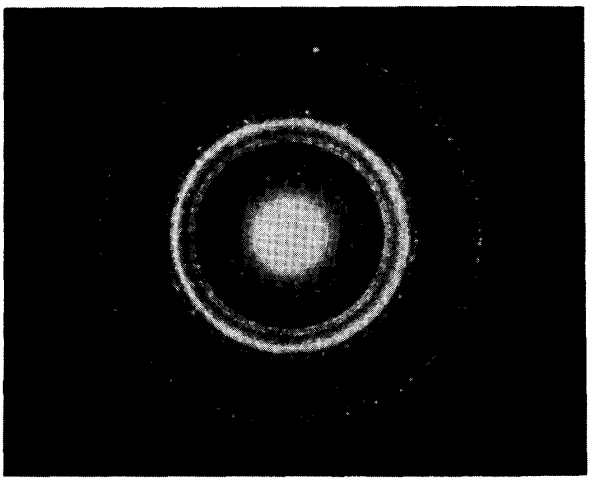

Fig. 7 Diffraction Pattern from the $Ti_{70}Fe_{20}B_{10}$ alloy annealed for 1800 s at 858 K. Analysis of this pattern is shown in Table II.

alloy samples indicated that a metastable b.c.c. supersaturated solid solution formed when annealed at T_{x1}, while the cubic Ti_2X (X= Fe, Co or Ni) intermediate phase precipitated when annealed at T_{x2}. This sequence justifies the interpretation from the D.T.A. curves that crystallization is a two-stage process in the present amorphous alloys. Continuous heating, on the other hand, indicated that an f.c.c. phase formed from the amorphous phase.

Now, we would like to discuss the formation of the metastable

Table II Analysis of the Diffraction Pattern from the $Ti_{70}Fe_{20}B_{10}$ alloy annealed for 1800 s at 858 K (Fig. 7).

S.No.	$d_{obs.}$ (nm)	Ti_2Fe		TiB	
		$d_{cal.}$ (nm)	hkl	$d_{cal.}$ (nm)	hkl
1	0.6757	0.6540	111		
2	0.5068	0.5664	200 ?		
3	0.3978	0.4006	220		
4	0.3448	0.3416	311		
5	0.3103			0.3053	200
6	0.2599	0.2599	331		
7	0.2472	0.2533	420	0.2543	201,011
8	0.2282	0.2312	422		
9	0.2191			0.2161	210
10	0.2111			0.2140	102
11	0.1968			0.1956	211
12	0.1843			0.1863	301
13	0.1725	0.1728	533		
14	0.1571	0.1571	640		
15	0.1458			0.1461	401
16	0.1351			0.1362	220,410
17	0.1299	0.1299	662	0.1310	411,221
18	0.1228	0.1236	842	0.1244 0.1219	122,213 303
19	0.1128			0.1141	004
20	0.1084			0.1079	502,403

f.c.c. phase observed in the in-situ annealed amorphous foils and not detected in samples heat treated externally. As mentioned earlier, the f.c.c. phase was found to have a lattice parameter of a = 0.46 nm. Table III lists the observed interplanar spacings and the Miller indices of this phase. Since we were unable to detect this phase in the externally heat treated samples, it was decided to perform a careful diffraction study of an in-situ annealed sample transferred to the 200 kV microscope. In most of the regions, we detected the same phase (f. c.c., a = 0.46 nm), but, at a few places we were able to get diffraction patterns, a typical of which is shown in Fig. 9. The interplanar spacings calculated from this pattern are also shown in Table III along with the visually estimated intensitites. It is important to note that

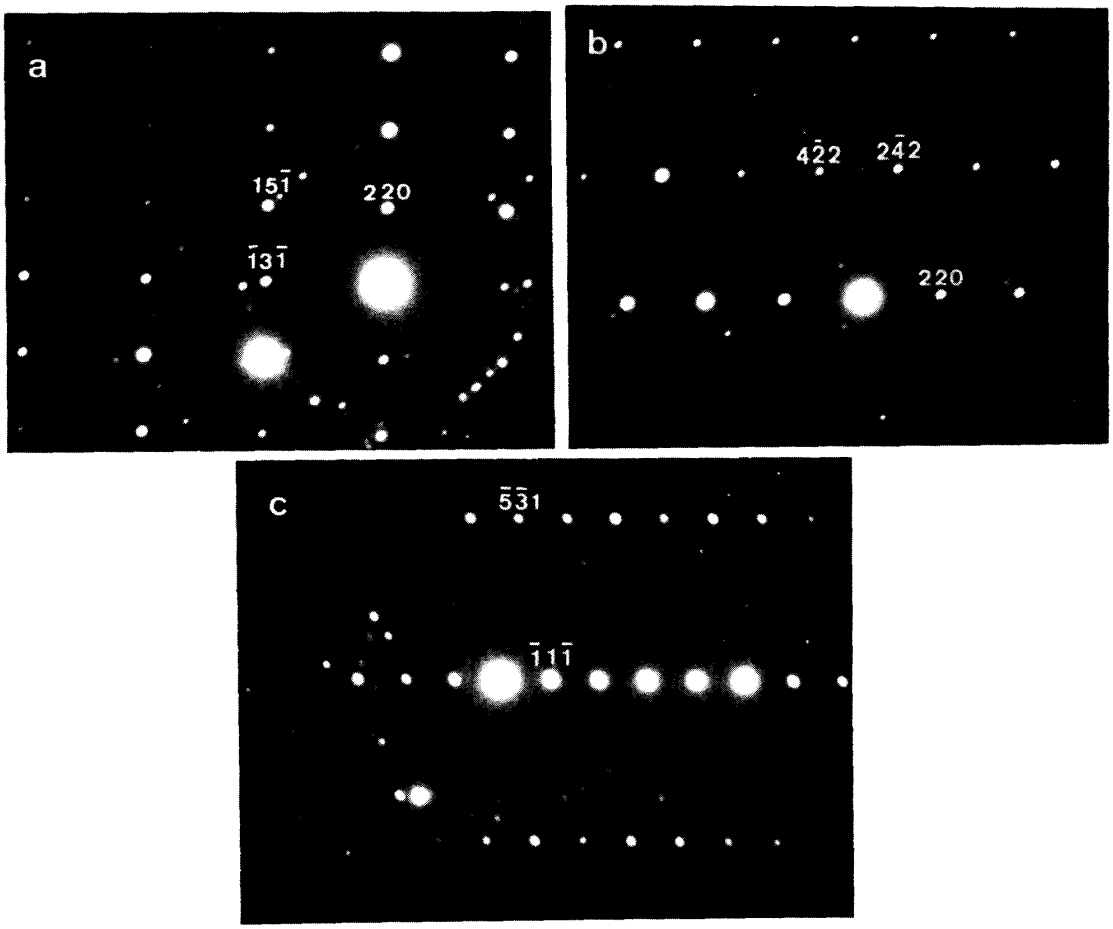

Fig. 8 Single-crystal Diffraction Patterns from the Ti_2Ni phase in annealed $Ti_{70}Ni_{20}B_{10}$ alloy. (a) [$\bar{1}$14], (b) [$\bar{1}$13] and (c) [1$\bar{3}\bar{4}$] orientations.

all the interplanar spacings observed in Fig. 3 b are also present here; however, more spacing could be observed in Fig. 9. All the interplanar spacings of Fig. 9 could be indexed on the basis of the equilibrium Ti_2Fe compound having an f.c.c. structure with a = 1.147 nm. This value of the lattice parameter is slightly larger than the equilibrium value of 1.133 nm. Further, the intensities of the observed reflections also match very well with those expected for the Ti_2Fe phase. These facts lead us to believe that the phase detected in the in-situ crystallized sample also is the same Ti_2X phase, but perhaps because of insufficient scattering effects, enough diffraction lines could not be recorded. Only the intense reflections were recorded.

From the foregoing it can be concluded that the general sequence of decomposition for the Ti-X-B (X=Fe, Co or Ni) amorphous alloys can be represented as:

Table III Interplanar Spacings and Visually estimated intensities corresponding to Diffraction patterns shown in Fig. 3 b and Fig. 9.

Fig. 3b				Fig. 9			
d(nm)	hkl	$I_{obs.}$	I^*_{Cu}	d(nm)	hkl	$I_{obs.}$	$I/I_o(Ti_2Co)$*
				0.4026	220	ms	-
				0.3215	222	w	30
0.2644	111	ms	100	0.2684	331	m	40
0.2244	200	vs	46	0.2271	333	vs	100
0.1627	220	w	20	0.1628	444	w	10
0.1397	311	vw	17	0.1429	800	vw	10
0.1329	222	vvw	5	0.1302	840	vvw	-
0.1157	400	vvw	3	-	-	-	-
0.1043	331	vvw	9	0.1023	953	vvw	-
f.c.c., a = 0.46 nm				f.c.c., a = 1.147 nm			

* From ASTM cards

vs: very strong, ms: medium strong m: medium, w: weak, vw: very weak, vvw: very very weak.

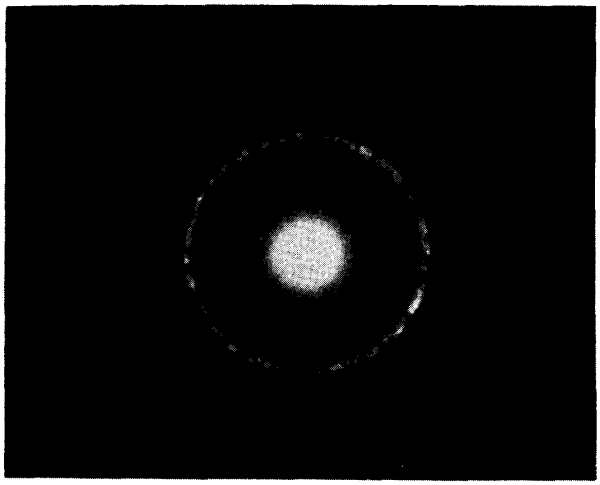

Fig. 9 Electron diffraction pattern of the $Ti_{70}Fe_{20}B_{10}$ alloy crystallized in-situ in the 100 kV microscope and observed in the 200 kV microscope. Analysis of this pattern is shown in Table III.

$$\text{Amorphous} \longrightarrow \text{Amorphous'} + \text{MS I} \longrightarrow \text{MS I} + \text{Intermediate Phase } Ti_2X \longrightarrow \text{Stable phases}$$

This mode of decomposition represented above is followed in almost all the amorphous alloys studied so far [12a].

IV. Conclusions

Amorphous alloys based on the composition $Ti_{70}X_{20}B_{10}$ (X=Fe, Co or Ni) could be produced by rapidly quenching their melts using a melt spinning technique. Detailed microscopic investigations have been carried out to follow the decomposition behavior. The first stage was the formation of a b.c.c. supersaturated solid solution and the second was the precipitation of the Ti_2Co compound. Further annealing produced the equilibrium phases in all the alloys.

Acknowledgement

One of the authors (C. S.) is grateful to the Japan Society for the Promotion of Science for financial assistance.

References

(1) 'Metallic Glasses', (eds.) J. J. Gilman and H. J. Leamy (American Society for Metals, Metals Park, Ohio), 1978.
(2) 'Rapidly Quenched Metals III', (ed.) B. Cantor (The Metals Society, London), 1978.
(3) 'Structure and Properties of Amorphous Metals', (eds.) T. Masumoto and K. Suzuki, Supplement to Sci. Rep. RITU, A27 (1978).
(4) T. Masumoto, K. Hashimoto and H. Fujimori, Sci. Rep. RITU, A25 (1975), 232.
(5) J. J. Gilman, Metal Progress, 116, No. 7 (1979), 42.
(6) T. F. Fedorov and Yu. B. Kuz'ma, Inorganic Materials, 3 (1967), 1307.
(7) Yu. B. Kuz'ma, Inorganic Materials, 7 (1971), 452.
(8) Yu. B. Kuz'ma and M. V. Chepiga, Soviet Powder Met. Met. Ceramics, 10 (1969), 832.
(9) A. Inoue, S. Sakai, H. M. Kimura and T. Masumoto, Trans. Japan Inst. Metals, 20 (1979), 255.
(10) R. A. Spurling, Metall. Trans. A6 (1975), 1660.
(11) quoted in D. E. Polk, A. Calka and B. C. Giessen, Acta Metall., 26 (1978), 1097.

(12) a. C. Suryanarayana, A. Inoue and T. Masumoto; b. A. Inoue, H. M. Kimura, S. Sakai and T. Masumoto, Papers to be presented at the Fourth International Conference on Titanium, Kyoto, Japan, May 1980.

(13) C. Suryanarayana, A. Inoue and T. Masumoto, Unpublished Research.

(14) T. Masumoto and R. Maddin, Acta Metall., 19 (1971), 725.

(15) A. Inoue, T. Masumoto, M. Kikuchi and T. Minemura, Sci. Rep. RITU, A27 (1979), 127.

(16) T. Masumoto, H. Kimura, A. Inoue and Y. Waseda, Mater. Sci. & Engg., 23 (1976), 141.